Available online at www.sciencedirect.com

SciVerse ScienceDirect

Ceramics International 39 (2013) 6777–6786

CERAMICS INTERNATIONAL

www.elsevier.com/locate/ceramint

Phase analysis and wear behavior of *in-situ* spark plasma sintered Ti_3SiC_2

Nidul C. Ghosh, Sandip P. Harimkar*

School of Mechanical and Aerospace Engineering, Oklahoma State University, Stillwater, OK 74078, USA

Received 25 January 2013; received in revised form 28 January 2013; accepted 2 February 2013
Available online 20 February 2013

Abstract

In-situ synthesis of dense near-single phase Ti_3SiC_2 ceramics from 3Ti/SiC/C/0.15Al starting powder using spark plasma sintering (SPS) at 1250 °C is reported. Systematic analysis of the phase development over a range of sintering temperatures (1050–1450 °C) suggested that solid state reactions between intermediate TiC and Ti_5Si_3 phases lead to the formations of Ti_3SiC_2. The effect of starting powder composition on phase development after SPS at 1150 °C was also investigated using three distinct compositions (3Ti/SiC/C, 2Ti/SiC/TiC, and Ti/Si/2TiC). The results indicate that the starting powder compositions, with higher amounts of intermediate phase such as TiC, favor the formation of Ti_3SiC_2 at relatively lower sintering temperature. Detailed analysis of wear behavior indicated that samples with higher percentage of TiC, present either as an intermediate phase or a product of Ti_3SiC_2 decomposition, exhibited higher microhardness and better wear resistance compared to near single phase Ti_3SiC_2.

Keywords: A. Sintering; B. Microstructure; C. Hardness; C. Wear resistance; D. Carbides

1. Introduction

Ti_3SiC_2 is a representative member of a family of layered ternary phases called as $M_{n+1}AX_n$ phases (M is a transition metal; A is an A group (mostly IIIA and IVA) element; X is C and/or N; and $n=1$–3) [1]. The presence of metallic, covalent, and ionic type chemical bondings in Ti_3SiC_2 gives the material remarkable combinations of properties of metallic and ceramic materials [2]. These materials are often referred to as "ductile ceramics" and exhibit properties such as lower density, high melting point, excellent electrical and thermal conductivity, good machinability, thermal shock resistance, damage tolerance, and fatigue, creep and high temperature oxidation resistance [3–5].

Ti_3SiC_2 was first synthesized by Jeitschko and Nowotny via chemical reaction between TiH_2, Si, and graphite in 1967 [6]. Over the years from 1967 to present, several methods, including magnetron sputtering [7], arc melting and post-annealing [8], chemical vapor deposition (CVD), pulsed laser deposition (PLD) [9], self-propagating high temperature synthesis (SHS) [10], mechanical alloying [11], and combustion synthesis with hot isostatic pressing [12], were employed for Ti_3SiC_2 synthesis. However, these processes almost always result in the formation of Ti_3SiC_2 accompanied with large amounts of undesired ancillary phases like TiC, Ti_5Si_3, and $TiSi_2$. Barsoum et al. synthesized almost single phase Ti_3SiC_2 from Ti, graphite, and SiC powders by employing hot isostatic pressing (HIP) at 1600 °C [13]. In the recent years, a novel solid state consolidation technique spark plasma sintering (SPS), where uniaxial compaction pressure is applied to the powder along with pulse direct current, was employed for synthesis of nanostructured/ultra-fine grained materials, difficult-to-sinter materials, and metastable/non-equilibrium phases. SPS presents tremendous potential for the processing of fully dense materials at relatively lower sintering temperature and in shorter sintering time without significant grain growth compared to conventional hot pressing [14]. SPS of Ti_3SiC_2 from Ti/Si/TiC [15,16], Ti/Si/C [17], Ti/SiC/TiC [18], Ti/$TiSi_2$/TiC [19], TiH_2/SiC/C [20] starting powder has been reported. However, similar sintering process applied to Ti/SiC/C starting composition

*Corresponding author. Tel.: +1 405 744 5830.
E-mail address: sandip.harimkar@okstate.edu (S.P. Harimkar).

0272-8842/$ - see front matter © 2013 Elsevier Ltd and Techna Group S.r.l. All rights reserved.
http://dx.doi.org/10.1016/j.ceramint.2013.02.008

resulted in the formation of Ti_3SiC_2 with higher amount of ancillary TiC (nearly 10%) [21]. Excess Si in starting composition was used to compensate for the evaporation of Si at higher temperature, resulting in decreased amount of ancillary TiC [22]. However, the higher percentage of Si content also resulted in appearance of a new ancillary phase, $TiSi_2$ [23]. Addition of small amount of aluminum in the starting powder is reported to favor the nucleation and growth of Ti_3SiC_2 [24]. In this paper, systematic investigation on the effect of sintering temperature, in the range of 1050–1450 °C, on the phase development during SPS of 3Ti/SiC/C/0.15Al powder is presented. The reaction mechanisms leading to formation of Ti_3SiC_2 and the possibility of formation of $Ti_3(Si_{1-x}Al_x)C_2$ solid solution during SPS are critically analyzed. Also, the effect of starting powder composition on phase development after SPS at 1150 °C is investigated using three distinct compositions (3Ti/SiC/C, 2Ti/SiC/TiC, and Ti/Si/2TiC). The effect of phase constituents in sintered Ti_3SiC_2 samples on the wear behavior (wear weight loss and coefficient of friction) is also presented.

2. Experimental procedure

Commercially available powders of Ti (< 44 μm), SiC (2–10 μm), graphite (< 44 μm), and Al (< 2 μm) were used for the synthesis of Ti_3SiC_2 phase. The starting powder, weighted according to molar ratio of Ti/SiC/C/Al (3:1:1:0.15), was milled for 1 h in a high energy planetary ball mill (Make: Fritsch; Model:Pulverisette 7). The mechanical milling was conducted using tungsten carbide milling media with an operating speed of 500 rpm and powder to ball ratio of 10:1. The ball milled powder was then compacted loosely in a 20 mm in diameter graphite die. The samples were then sintered using SPS in a temperature range of 1050–1450 °C with a uniaxial pressure of 50 MPa, soaking time of 15 min, and heating rate of 100 °C/min (Make: Thermal Technology, Inc.; Model: 10-3). To investigate the effect of starting powder composition on phase development, three different powder mixtures (3Ti–SiC–C, 2Ti–SiC–TiC and Ti–Si–2TiC) were also sintered using SPS at 1150 °C with a uniaxial pressure of 50 MPa and soaking time of 15 min. The phase constituents and microstructure of the ball milled powder and sintered samples were analyzed using X-ray diffractometer (Make: Philips Norelco; Model: PW1830) operating with CuK_α radiation ($\lambda = 1.54178$ Å) and Scanning Electron Microscope (SEM) (Make: JEOL; Model: JSM-633OF) equipped with energy dispersive X-ray spectroscopy (EDS) detector. Microhardness of the samples was measured using a Vickers hardness tester (Clark Instruments; Model: CM-700AT) operated with the normal force of 9.8 N and holding time of 15 s. About ten hardness readings were taken on each sample and the average value was reported along with positive and negative error bars. Wear tests were conducted using a ball-on-disk configuration (Make: Nonovea; Model: MT/60). Polished surfaces of 20 mm diameter sintered discs were slid against 6 mm diameter aluminum oxide (Al_2O_3) ball to form 4 mm diameter wear tracks on the surfaces. The wear tests were conducted with a normal force of 10 N and sliding velocity of 200 rpm. The wear weight loss data for the samples was recorded after every 10 min interval with total wear test duration of 1 h. The depth profiles across the wear tracks were measured out using a non-contact optical 3D profilometer (Make: Nanovea; Model: PS50).

3. Results and discussion

3.1. Analysis of phases in starting powder and spark plasma sintered samples

X-ray diffraction (XRD) patterns from ball milled powder (Ti/SiC/C/Al) and samples spark plasma sintered at different sintering temperatures in a range of 1050–1450 °C are presented in Fig. 1. The XRD pattern from the ball milled powder showed peaks corresponding to major constituents, Ti and SiC, in the starting composition. Note that the ball milling was conducted to mix the starting power uniformly and not to initiate any new phase formation. The SPS sintering with the investigated processing parameters (temperature range of 1050–1450 °C, uniaxial pressure of 50 MPa, and soaking time of 15 min) resulted in *in-situ* reactions forming new phases. The peaks corresponding to starting constituents Ti and SiC were absent in the XRD patterns of all the sintered samples. For the samples sintered at relatively lower temperatures (1050–1150 °C), the peaks corresponding to new phases, TiC and Ti_5Si_3, were observed in the XRD patterns. In this temperature range, Ti seems to react with free C and SiC to form TiC and Ti_5Si_3. The XRD pattern indicated the

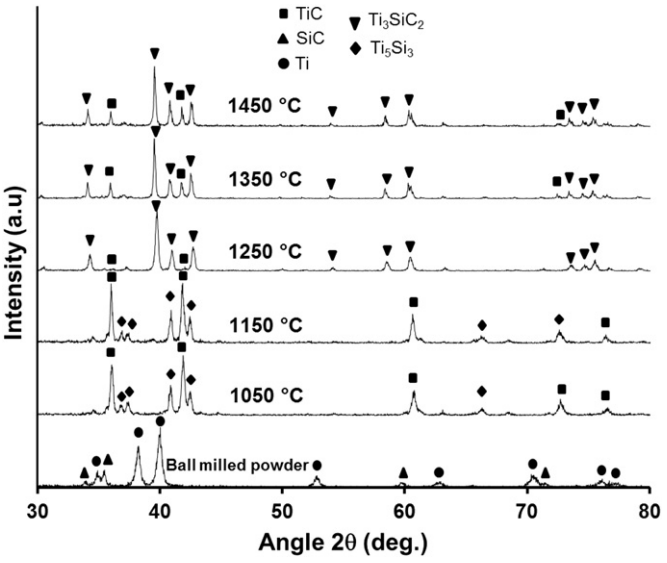

Fig. 1. X-ray diffraction patterns from ball milled 3Ti/SiC/C/0.15Al powder mixture and samples spark plasma sintered at 1050 °C, 1150 °C, 1250 °C, 1350 °C, and 1450 °C.

formation of Ti_3SiC_2 at the intermediate sintering temperature of 1250 °C. Although some peaks of TiC can still be observed in the XRD pattern for the sample at this temperature (1250 °C), the intensity of TiC peaks was much lower compared to that for Ti_3SiC_2 peaks. With further increase in sintering temperature to 1350–1450 °C, the intensity of the TiC peaks increased again indicating increasing content of minor phase TiC with increasing sintering temperature.

The quantitative analysis to determine the amounts of different phases present in the spark plasma sintered samples was conducted using experimentally calibrated standard additive method developed by Zou et al. [25]. According to this method, the weight percentages (W) of three major phases, TiC, Ti_5Si_3, and Ti_3SiC_2, are given by

$$W_{TiC} = \frac{I_{TiC}}{1.222I_{Ti_3SiC_2} + 5.084I_{Ti_5Si_3} + I_{TiC}} \quad (1)$$

$$W_{Ti_5Si_3} = \frac{I_{Ti_5Si_3}}{0.240I_{Ti_3SiC_2} + I_{Ti_5Si_3} + 0.197I_{TiC}} \quad (2)$$

$$W_{Ti_3SiC_2} = \frac{I_{Ti_3SiC_2}}{I_{Ti_3SiC_2} + 4.159I_{Ti_5Si_3} + 0.818I_{TiC}} \quad (3)$$

where I_{TiC}, $I_{Ti_5Si_3}$, and $I_{Ti_3SiC_2}$ are the intensities of TiC, Ti_5Si_3, and Ti_3SiC_2 phases, respectively. The intensities of sharp non-overlapping peaks, (111) for TiC, (102) for Ti_5Si_3, and (104) for Ti_3SiC_2 phases, were used for the quantitative analysis. Fig. 2 shows the variation of calculated weight percentages of TiC, Ti_5Si_3, and Ti_3SiC_2 phases in the spark plasma sintered samples with sintering temperature (1050–1450 °C). The samples sintered at 1050 °C consisted of about 50 wt% Ti_5Si_3 and about 50 wt% TiC. There was slight increase in Ti_5Si_3 content to about 60 wt% with increase in temperature from 1050 to 1150 °C. The absence of Ti_3SiC_2 in the temperature range of 1050–1150 °C suggests that minimum sintering temperature required for Ti_3SiC_2 formation is above 1150 °C in accordance with Cordoba et al. [26] and Wu and Kisi. [27]. Near complete reaction leading to the formation of Ti_3SiC_2 phase (98.5 wt%) occurred at sintering temperature of 1250 °C. The only auxiliary phase present at this temperature (1250 °C) was TiC, suggesting complete consumption of Ti_5Si_3 in the process of Ti_3SiC_2 formation. These results are in agreement with the previous works of El-Raghy and Barsoum [28] and Arunajatesan and Carim [8] suggesting TiC and Ti_5Si_3 as the intermediate phases for the formation of Ti_3SiC_2 from Ti/SiC/C starting powder. Above SPS temperature of 1250 °C, the observed increasing amount of auxiliary TiC indicates decomposition of Ti_3SiC_2 into TiC at higher temperature. The calculated amount of TiC phase at the sintering temperature of 1450 °C was about 16%. With the investigated starting composition and processing parameters, the optimum temperature for near complete *in-situ* reaction and consolidation of Ti_3SiC_2 was found to be 1250 °C. SPS below or above this optimum temperature results in incomplete transformation or decomposition of Ti_3SiC_2 phase, respectively, forming undesirable auxiliary phases. The absence of Ti_5Si_3 in the samples sintered at and above 1250 °C is a clear indication of complete consumption of Ti_5Si_3 phase in the conversion to Ti_3SiC_2. It seems that the nucleation and subsequent growth of Ti_3SiC_2 phase occurred on Ti_5Si_3 crystals rather than TiC. While the nucleation of Ti_3SiC_2 on Ti_5Si_3 requires diffusion of C, its nucleation on TiC would involve diffusion of both Si and C atoms [28,29]. The low diffusion rate of Si in TiC-related system [30] and closer structural relationship between Ti_5Si_3 and Ti_3SiC_2 [31] suggests that Ti_3SiC_2 is more likely to nucleate on Ti_5Si_3 instead of TiC crystals. Additional reaction mechanism often proposed involves formation of Ti–Si liquid phase and its subsequent reaction with TiC to form Ti_3SiC_2 [17,32,33]. The Ti–Si liquid phase could be either Ti–Ti_5Si_3 [34] or Ti–$TiSi_2$ [15,23] which form at a temperature of about 1333 °C [35]. In our experiments, optimum sintering temperature for forming Ti_3SiC_2 was found to be 1250 °C, which is significantly lower than the eutectic temperature of Ti–Si liquid phase (1333 °C). The formation of major liquid phase leading to formation of Ti_3SiC_2 could not be confirmed by neutron diffraction study of Ti–SiC–C system [27,36]. As such, the reaction leading to Ti_3SiC_2 phase formation seems to be primarily solid state reaction between TiC and Ti_5Si_3 rather than Ti–Si liquid phase formation. El-Raghy and Barsoum [28] also proposed the formation of intermediate phases and their conversion into Ti_3SiC_2 as simultaneous processes. In our experimental results, only TiC and Ti_5Si_3 phases were detected up to sintering temperature of 1150 °C suggesting Ti_3SiC_2 formation only after complete formation of intermediate TiC and Ti_5Si_3 phases.

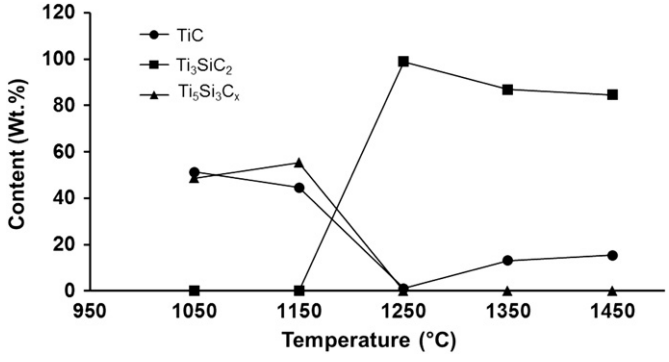

Fig. 2. Variation of Ti_3SiC_2, Ti_5Si_3, and TiC phase content with SPS temperature.

As discussed, an increasing amount of auxiliary TiC was observed in the samples sintered above 1250 °C. Ti_3SiC_2 became unstable and decompose at higher temperatures according to the reaction [1]:

$$M_{n+1}AX_n \rightarrow M_{n+1}X_n + A \quad (4)$$

As Ti_3SiC_2 has sandwich like structure with Ti–C blocks separated by hexagonal nets of Si, the decomposition of Ti_3SiC_2 is initiated by the loss of Si. Ti_3SiC_2 was reported

to be thermodynamically stable up to 1600 °C in vacuum or Ar atmosphere for 24 h [28]. However, the decomposition kinetics of Ti_3SiC_2 is highly dependent on the surrounding medium of Ti_3SiC_2. The presence of C act as a driving force for increasing Si segregation causing decomposition of Ti_3SiC_2 at temperatures lower than 1600 °C, according to the reaction [37]:

$$Ti_3SiC_2 \rightarrow 3TiC_{0.67}(s) + Si(g) \quad (5)$$

During SPS, contacting surfaces of graphite dies and punch with the sample provide carbon medium, resulting in decomposition of Ti_3SiC_2 into TiC_x at temperatures 1350 and 1450 °C primarily at the sample surfaces. By means of inward diffusion of C, Si planes of Ti_3SiC_2 are replaced by C planes, forming TiC_x layers on the surface [38]. Racault et al. [37] also suggested formation of SiC from free Si and C, according to the reaction: Si(g)+C→SiC. The XRD and SEM micrographs of the samples sintered above 1300 °C confirmed absence of any SiC on the surface layer. Thus, the free Si seems to have escaped from the surface of the samples rather than forming SiC. This also explains the observation of weight loss when Ti_3SiC_2 was heated in C crucibles above 1300 °C [37].

3.2. Effect of starting powder composition on phase development

XRD patterns from the samples sintered using SPS from three different powder mixtures (3Ti–SiC–C, 2Ti–SiC–TiC and Ti–Si–2TiC) are presented in Fig. 3. The figure indicates that no Ti_3SiC_2 phase was formed in samples sintered from starting composition of 3Ti–SiC–C at this temperature (1150 °C). However, the peaks corresponding to Ti_3SiC_2 phase were detected for the samples sintered from 2Ti–SiC–TiC and Ti–Si–2TiC compositions. Intense Ti_3SiC_2 peaks were observed for samples sintered from Ti–Si–2TiC composition. The relative amounts of Ti_3SiC_2 calculated using

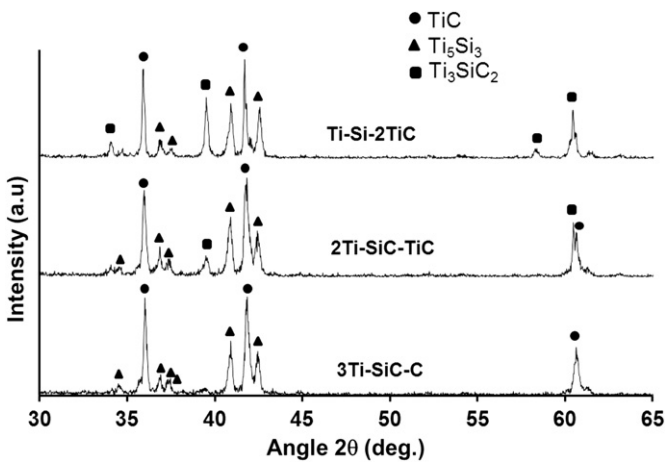

Fig. 3. X-ray diffraction patterns from samples spark plasma sintered at 1150 °C using three different powder compositions (3Ti/SiC/C, 2Ti/SiC/TiC, and Ti/Si/2TiC).

standard additive method (Eq. (3)) were found to be 0%, 13.18%, and 39.85% for compositions 3Ti–SiC–C, 2Ti–SiC–TiC, and Ti–Si–2TiC, respectively. These results clearly indicate that increasing amount of Ti_3SiC_2 can be formed in the spark plasma sintered product at lower sintering temperatures from starting compositions with increasing amounts of TiC. In Ti/SiC system, intermediate TiC phase is formed first due to its higher thermodynamic stability, according to the reaction [28]:

$$SiC + Ti \rightarrow TiC + Si, \quad \Delta G^{\circ} = -107\ \text{KJ}\ (1000\ ^{\circ}C) \quad (6)$$

The released Si then reacts with Ti forming another intermediate phase Ti_5Si_3, according to reaction

$$5Ti + 3Si \rightarrow Ti_5Si_3, \quad \Delta G^{\circ} = -590\ \text{KJ}\ (1000\ ^{\circ}C) \quad (7)$$

As the Gibbs free energy changes are negative for these reactions, the formation of intermediate phases TiC and Ti_5Si_3 is favored [31]. The intermediate phases TiC and Ti_5Si_3 start to form simultaneously at low temperatures. The desired Ti_3SiC_2 phase forms when the constitutions of TiC and Ti_5Si_3 phases are completed (Fig. 2). The addition of TiC in the starting powder seems to favor the completion of Ti_5Si_3 constitution at lower temperature resulting in subsequent formation of Ti_3SiC_2. Similarly, addition of Si instead of SiC in the starting powder seems to favor formation of intermediate phase Ti_5Si_3 through reaction (7) skipping reaction (6). Thus, the starting compositions containing TiC and Si favor the complete formation of intermediate phases and subsequent formation of Ti_3SiC_2 at lower sintering temperatures.

3.3. Analysis of microstructure in spark plasma sintered samples

SEM micrographs of polished and etched surfaces of samples sintered from Ti/SiC/C/Al powder mixture are presented in Fig. 4. When the sintering temperature was 1050 °C, only TiC and Ti_5Si_3 were observed in micrographs (Fig. 4(a)). As the HF based etching solution dissolves silicides, the Ti_5Si_3 phase appears corroded in the micrographs [8]. At 1250 °C, a duplex microstructure of plate shaped grains (3–5 μm in length and 1–2 μm in width) and fine equiaxed grains (1–3 μm in diameter) with some dispersed bright spots was observed (Fig. 4(b)). The size of the plate shaped grains increased with increasing sintering temperature. The size of plate shaped grains was about 5–15 μm in length and 2–5 μm in width for the sintering temperature of 1450 °C (Fig. 4(c)). EDS spot analysis was performed at the plate shaped grain (point 1), the bright spot (point 2), and the fine equixed grain (point 3) of the sample sintered at 1250 °C (Fig. 5). With the EDS detector used, only Ti, Si, and Al peaks could be detected. From the corresponding peaks of Ti, Si, and Al, the plate shaped grains (point 1) and equiaxed grains (point 3) seem to be Ti_3SiC_2. The XRD analysis also indicated Ti_3SiC_2 as a major phase at this sintering temperature (Fig. 1). Intense peaks of Al and Si were

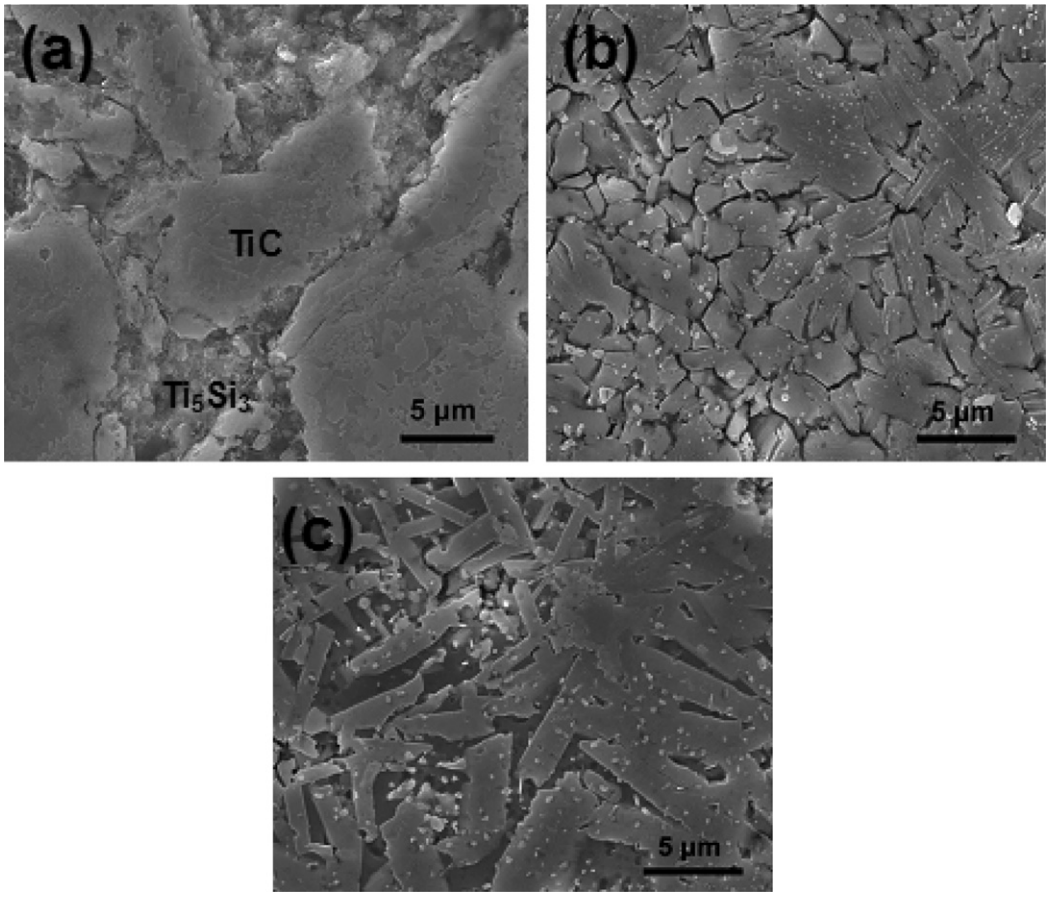

Fig. 4. SEM micrographs of samples spark plasma sintered from 3Ti/SiC/C/0.15Al powder at (a) 1050 °C, (b) 1250 °C, and (c) 1450 °C.

observed for the bright grain (point 2) and it seems to be a solid solution of Ti_3SiC_2 and Al, $Ti_3(Si_{1-x}Al_x)C_2$. El-Raghy and Barsoum [28] reported formation of single phase Ti_3SiC_2 ($>99\%$) from Ti–SiC–C starting composition using hot isostatic pressing (HIP) in the temperature range of 1450–1600 °C. The grain size of Ti_3SiC_2 samples, hot pressed at 1600 °C for 4 h, was found to be about 100–200 μm. Clearly, the above results indicate that near single phase Ti_3SiC_2 (98.5%) with finer microstructure can be formed at relatively lower sintering temperature (1250 °C) and shorter holding time (15 min) using SPS compared to HIP and other conventional sintering technique [4,39]. Zhang et al. [23] reported synthesis of Ti_3SiC_2 from Ti/SiC/C (3:1:1) powders using SPS, but only 50% or less Ti_3SiC_2 was formed over wide ranges of sintering temperature and time. With the addition of 0.15 mol of aluminum in stoichiometric Ti/SiC/C (3:1:1) composition, near single phase Ti_3SiC_2 (98.5%) was observed for samples spark plasma sintered at 1250 °C (Fig. 2). At the SPS temperature (1250 °C), the aluminum powder (melting point of 660 °C) forms interfacial liquid phase favoring diffusion of Ti and C atoms for Ti_3SiC_2 formation. It was recently reported that the addition of small amount of aluminum during the synthesis of Ti_3SiC_2 removes the impurity TiC by forming solid solution of $Ti_3(Si_{1-x}Al_x)C_2$ [40]. To analyze the possibility of solid solution formation, EDS mapping of aluminum for the sample sintered at 1250 °C was conducted (Fig. 6). The EDS elemental mapping shows that the distribution of aluminum was non-uniform with some distributed aluminum-rich regions. These aluminum-rich regions corresponded with bright spots in the SEM micrographs. Spot EDS at these regions (point 2 in Fig. 5) also showed presence of both Al and Si along with Ti, suggesting formation of $Ti_3(Si_{1-x}Al_x)C_2$ solid solution. Addition of excess Al in starting composition is also expected to induce reaction between Ti and Al forming compounds such as Ti_3AlC_2 and Ti_3Al. No such phases were detected in the XRD patterns precluding the possibility of excess aluminum addition.

3.4. Microhardness and wear behavior

The microhardness of samples spark plasma sintered at 1250 °C was found to be 6.32 ± 0.17 GPa. The value reported in the literature for pure Ti_3SiC_2 was nearly 4 GPa [41]. Note that these samples contained about 98.5% Ti_3SiC_2 with TiC as minor impurity phase. Relatively higher hardness observed in the present investigation could be due to lower indentation load, finer microstructure, and presence of hard impurity phase (1.5% TiC).

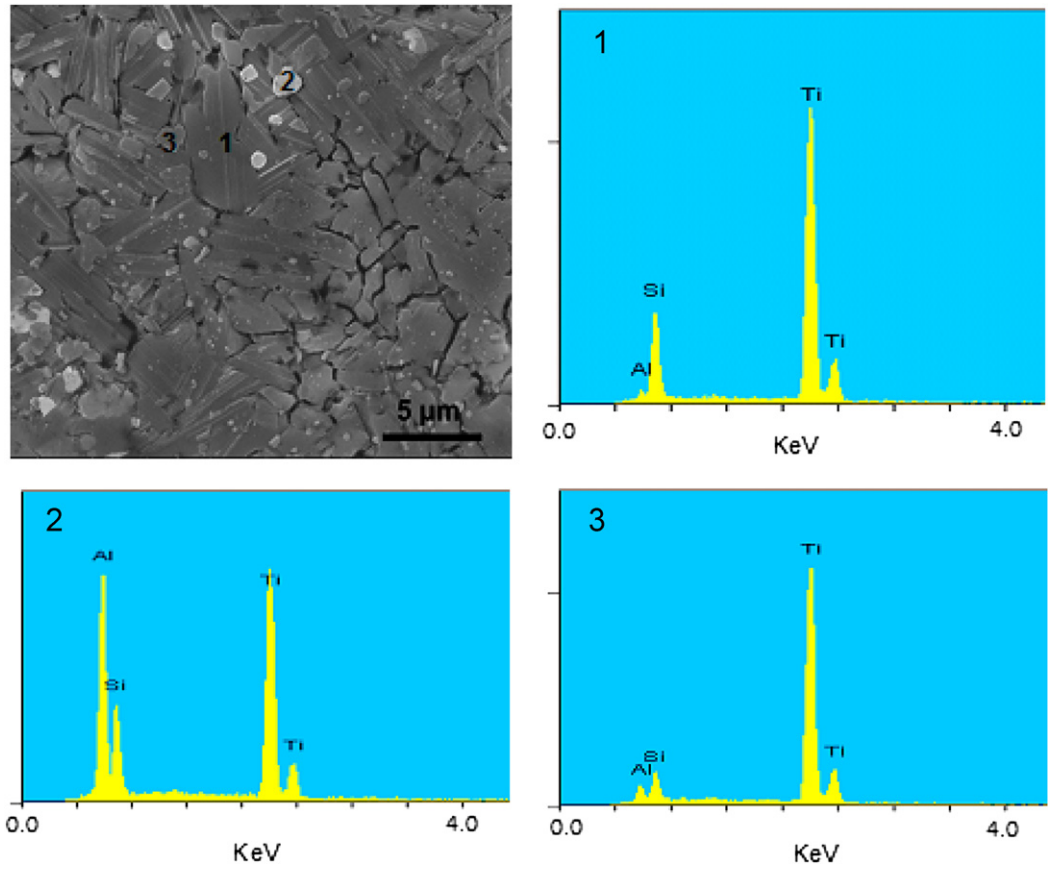

Fig. 5. EDS elemental analysis of different phase regions of sample spark plasma sintered at 1250 °C.

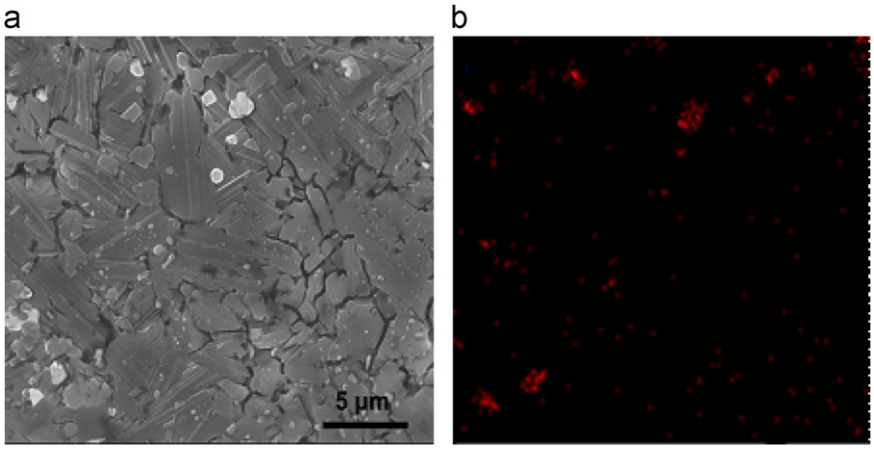

Fig. 6. EDS elemental mapping of aluminum for sample spark plasma sintered at 1250 °C.

At lower indentation loads, the values represent the hardness of single crystal as the indentation is within one grain. El-Raghy and Barsoum [41] reported that hardness becomes independent of indentation load and grain size at higher loads (100 N). The samples sintered at 1350 °C and 1450 °C exhibited hardness of 6.83 ± 0.12 GPa and 7.05 ± 0.21 GPa, respectively. The higher hardness values for these samples sintered at 1350 and 1450 °C seems to be primarily due to presence of higher percentage (13–15%) of hard TiC phase in the microstructure.

Cumulative wear weight loss as a function of sliding time during ball-on-disc wear testing for samples sintered at 1050, 1250, and 1450 °C are presented in Fig. 7. The samples sintered at 1250 °C and 1050 °C exhibited highest and lowest wear weight loss, respectively. The samples sintered at 1450 °C showed intermediate values

of cumulative weight loss. This trend can be explained based on the variation of TiC content in the final sintered microstructure. As discussed earlier (Fig. 2), the samples sintered at 1250 °C contained lowest percentage of TiC (~1.5%) while those sintered at 1050 °C sample contained 51.25% TiC. The samples sintered at 1450 °C contained nearly 16% TiC. As TiC has significantly higher hardness (23.5 GPa) compared to Ti_3SiC_2 (6 GPa), the normal load on Ti_3SiC_2 during testing is effectively reduced with the presence of TiC. The harder TiC phase present in the microstructure seems to reduce ploughing or scrapping effect at the contact surfaces resulting in lower weight loss for samples with higher TiC content. The samples sintered at 1250 °C also showed wider wear track with average depth of wear track of about 50–60 μm. The average depths of wear track for samples sintered at 1050 and 1450 °C were about 10 and 20 μm, respectively (Fig. 8). The cumulative wear weight loss and the wear depth follow inverse relation with hardness of the sintered samples in agreement with the Archard's relationship. Fig. 9 shows the variation of coefficient of friction during each 10 min interval for the entire duration of wear test (60 min) for the samples sintered at 1050, 1250, and 1450 °C. During first 10 min interval, the coefficient of friction increases rapidly and stabilizes to steady state value for each sample. Note that most of the wear weight loss was observed in the first 10 min interval of the wear test. The weight loss seems to initiate with the two-body abrasive wear mechanism in the first interval causing sudden increase in coefficient of friction. After this initial stage, the formed wear debris seems to cause three-body abrasive wear at the contacting surfaces for rest of the wear tests (all test intervals). The average coefficient of friction for the samples sintered at 1250 °C and 1450 °C was about 0.85 (Fig. 9(d)). The average coefficient of friction was relatively lower (~0.6) for samples sintered at 1050 °C. This can be attributed to the very high amount (~51%) hard TiC phase in these samples. The SEM micrographs of the worn out surfaces of spark plasma sintered samples are presented in Fig. 10. The worn surfaces of the samples sintered at 1050 and 1450 °C were relatively flatter (see for example, the elevated flatter region on left of Fig. 10(a) and on right of Fig. 10(c)) than those for samples sintered at 1250 °C. However, major cracks separate the elevated flatter surface features from rougher depressed regions covered with fine wear debris. The worn surface from the samples sintered at 1250 °C exhibited numerous flat elevated features and debris-filled depressed regions with micro-cracks leading to debris-filled regions.

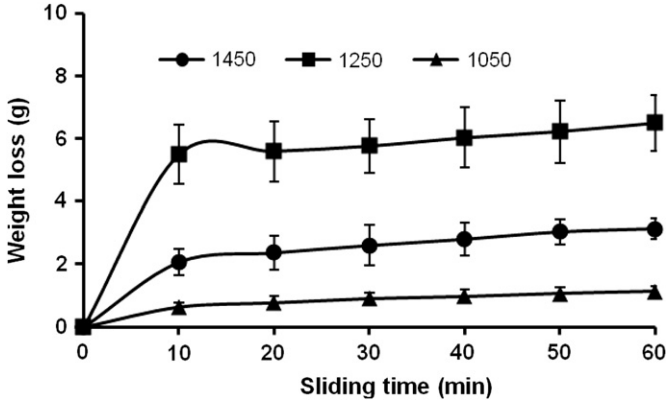

Fig. 7. Cumulative wear weight loss as a function of sliding time for samples spark plasma sintered at 1050 °C, 1250 °C, and 1450 °C.

4. Conclusions

Nearly single phase dense Ti_3SiC_2 was consolidated *in-situ* from 3Ti/SiC/C/0.15Al powder mixture using spark plasma sintering at 1250 °C. At lower sintering

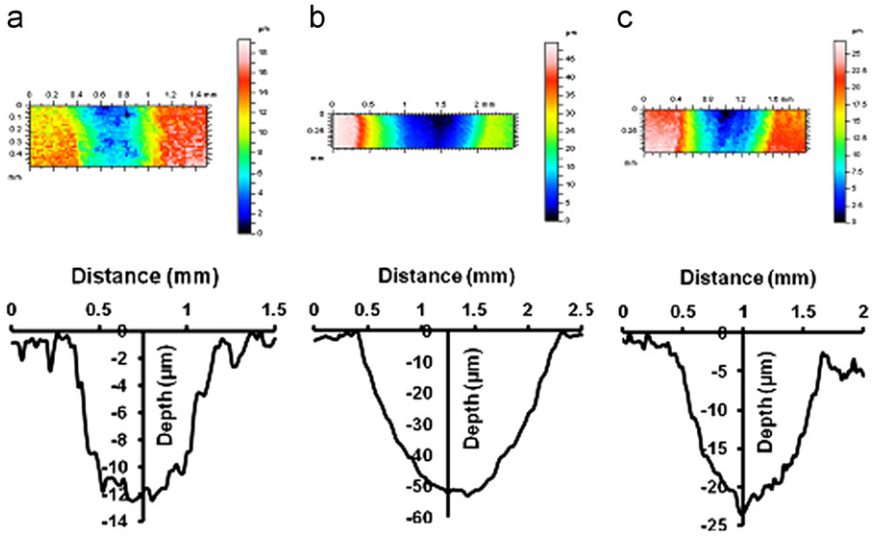

Fig. 8. Depth profiles across the wear tracks for samples spark plasma sintered at (a) 1050 °C, (b) 1250 °C, and (c) 1450 °C.

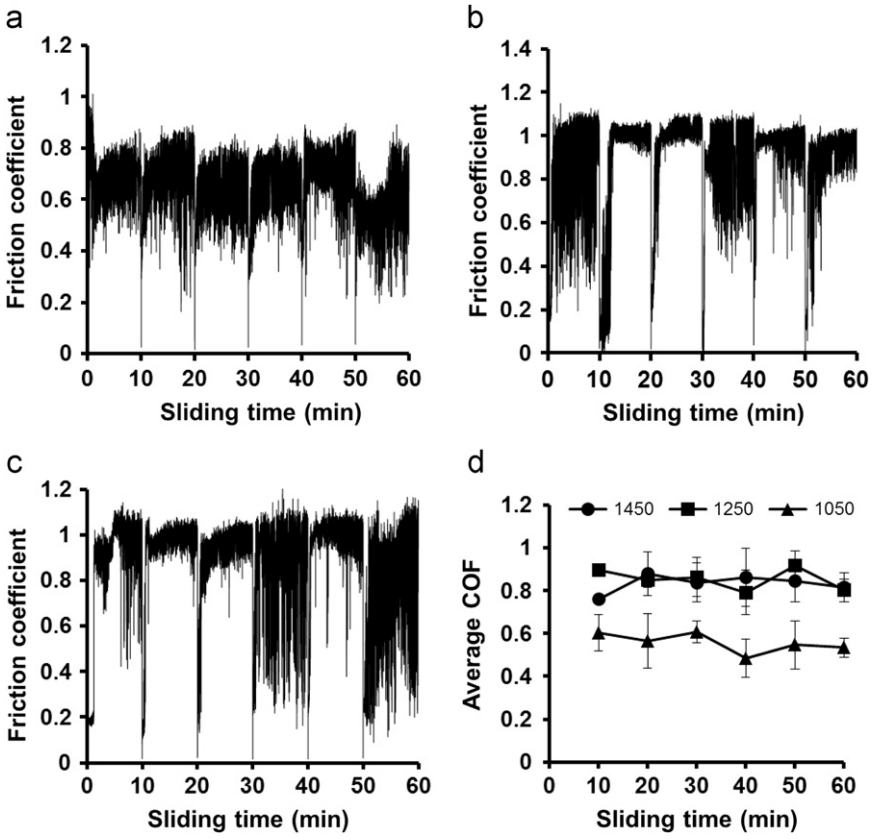

Fig. 9. Variation of coefficient of friction with sliding time for samples spark plasma sintered at (a) 1050 °C (b) 1250 °C, and (c) 1450 °C; (d) comparison of average coefficient of friction for samples spark plasma sintered at three different temperatures.

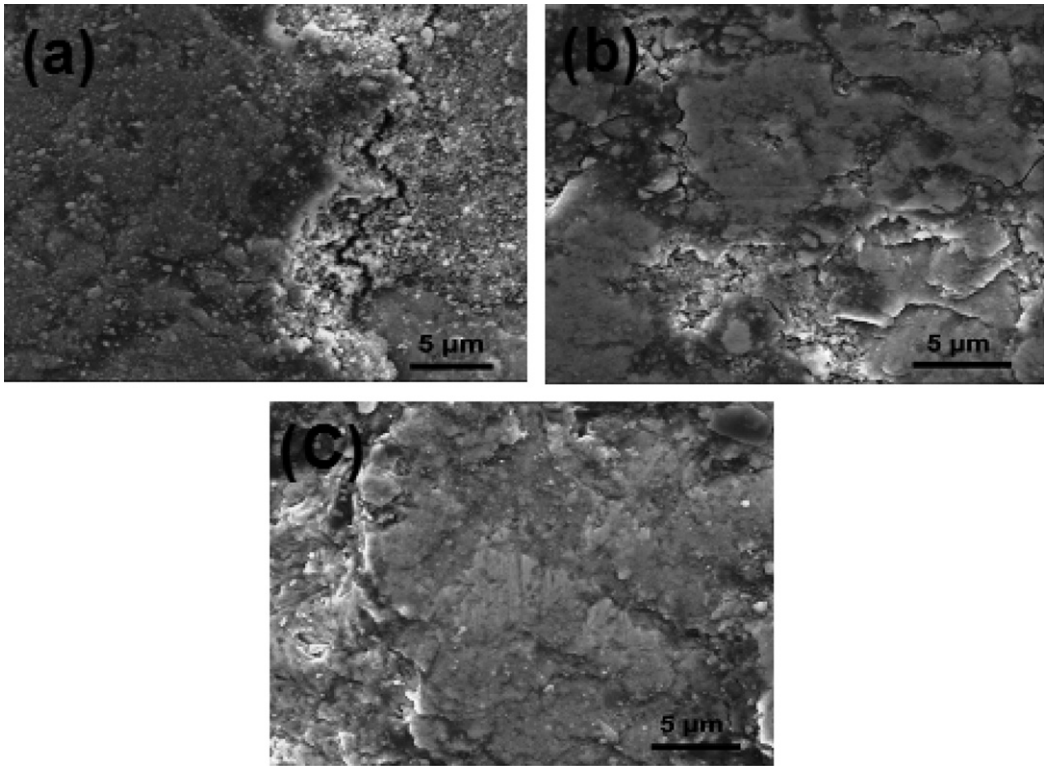

Fig. 10. SEM micrographs from the worn surfaces of samples spark plasma sintered at (a) 1050 °C (b) 1250 °C, and (c) 1450 °C.

temperatures, formation of intermediate phases TiC and Ti_5Si_3 was observed. The formation of Ti_3SiC_2 seems to initiate after complete constitution of intermediate phases. The stability of Ti_3SiC_2 decreases in presence of surrounding carbon medium at temperature above 1300 °C leading to decomposition of Ti_3SiC_2, forming auxiliary TiC phase. The starting powder compositions (2Ti/SiC/TiC and Ti/Si/2TiC) with higher amount of TiC (one of the intermediate phases) resulted in Ti_3SiC_2 formation at lower temperature compared to that with conventional 3Ti/SiC/C powder composition. The samples with higher percentage of TiC, either as an intermediate phase or the product of Ti_3SiC_2 decomposition, exhibited higher microhardness and better wear resistance than near single phase Ti_3SiC_2.

References

[1] M.W. Barsoum, The $M_{N+1}AX_N$ phases: a new class of solids; thermodynamically stable nanolaminates, Progress in Solid State Chemistry 28 (2000) 201–281.

[2] Y. Zhou, Z. Sun, Electronic structure and bonding properties in layered ternary carbide Ti_3SiC_2, Journal of Physics: Condensed Matter 12 (2000) 457–462.

[3] M.W. Barsoum, T. El-Raghy, C.J. Rawn, W.D. Porter, H. Wang, E.A. Payzant, C.R. Hubbard, Thermal properties of Ti_3SiC_2, Journal of Physics and Chemistry of Solids 60 (1999) 429–439.

[4] M.W. Barsoum, T. El-raghy, Synthesis and characterization of a remarkable ceramic: Ti_3SiC_2, Journal of the American Ceramic Society 79 (1996) 1953–1956.

[5] S.B. Li, J.X. Xie, L.T. Zhang, L.F. Cheng, Synthesis and some properties of Ti_3SiC_2 by hot pressing of Ti, Si and C powders. Part 2—mechanical and other properties of Ti_3SiC_2, Materials Science and Technology 21 (2005) 1054–1058.

[6] W. Jeitschko, H. Nowotny, Die kristallstructur von Ti_3SiC_2—ein neuer komplxcarbid-type, Monatshefte für Chemie 98 (1967) 329–337.

[7] J. Emmerlich, H. Hogberg, S. Sasvari, P.O.A. Persson, L. Hultman, J.P. Palmquist, et al., Growth of Ti_3SiC_2 thin films by elemental target magnetron sputtering, Journal of Applied Physics 96 (2004) 4817–4826.

[8] S. Arunajatesan, A.H. Carim, Synthesis of titanium silicon carbide, Journal of the American Ceramic Society 78 (1995) 667–672.

[9] J.J. Hu, J.E. Bultman, S. Patton, J.S. Zabinski, Pulsed laser deposition and properties of $M_{n+1}AX_n$ phase formulated Ti_3SiC_2 thin films, Tribology Letters 16 (2004) 113–122.

[10] J. Lis, R. Pampuch, Reaction sintering phenomena of self-propagating high temperature synthesis-derived ceramic powders in the Ti–Si–C system, Solid State Ionics 59 (1997) 101–103.

[11] S.B. Li, H.X. Zhai, Synthesis and reaction mechanism of Ti_3SiC_2 by mechanical alloying of elemental Ti, Si and C powders, Journal of the American Ceramic Society 88 (2005) 2092–2098.

[12] J. Lis, Y. Miyamoto, R. Pampuch, K. Tanihata, Ti_3SiC_2-based materials prepared by HIP–SHS techniques, Material Letters 22 (1995) 163–168.

[13] M.W. Barsoum, T. El-Raghy, Synthesis and characterization of a remarkable ceramic: Ti_3SiC_2, Journal of the American Ceramic Society 79 (1996) 1953–1956.

[14] Z.A. Munir, U. Anselmi-Tamburini, M. Ohyanagi, The effect of electric field and pressure on the synthesis and consolidation of materials: a review of the spark plasma sintering method, Journal of Materials Science 41 (2006) 763–777.

[15] Z.F. Zhang, Z.M. Sun, H. Hashimoto, Rapid synthesis of ternary carbide Ti_3SiC_2 through pulse-discharge sintering technique from Ti/Si/TiC powders, Metallurgical and Materials Transactions A 33 (2002) 3321–3328.

[16] N.F. Gao, J.T. Lib, D. Zhang, Y. Miyamoto, Rapid synthesis of dense Ti_3SiC_2 by spark plasma sintering, Journal of the European Ceramic Society 22 (2002) 2365–2370.

[17] Z.F. Zhang, Z.M. Sun, H. Hashimoto, T. Abe, Application of pulse discharge sintering (PDS) technique to rapid synthesis of Ti_3SiC_2 from Ti/Si/C powders, Journal of the European Ceramic Society 22 (2001) 2957–2961.

[18] Z.F. Zhang, Z.M. Sun, H. Hashimoto, T. Abe, A new synthesis reaction of Ti_3SiC_2 through pulse discharge sintering Ti/SiC/TiC powder, Scripta Materialia 45 (2001) 1461–1467.

[19] Z.F. Zhang, Z.M. Sun, H. Hashimoto, T. Abe, A new synthesis reaction of Ti_3SiC_2 from Ti/$TiSi_2$/TiC powder mixtures through pulse discharge sintering (PDS) technique, Materials Research Innovations 5 (2001) 185–189.

[20] Y. Zou, Z.M. Sun, S. Tada, H. Hashimoto, Synthesis reactions for Ti_3SiC_2 through pulse discharge sintering TiH_2/Si/TiC powder mixture, Materials Research Bulletin 43 (2008) 968–975.

[21] Z.M. SUN, H. Hashimoto, Z. Zhang, S. Yang, S. Tada, Synthesis and characterization of a metallic ceramic material—Ti_3SiC_2, Materials Transactions 47 (2006) 170–174.

[22] Z.F. Zhang, Z.M. Sun, H. Hashimoto, T. Abe, Effects of sintering temperature and Si content on the purity of Ti_3SiC_2 synthesized from Ti/Si/TiC powders, Journal of Alloys and Compounds 352 (2003) 283–289.

[23] Z.F. Zhang, Z.M. Sun, H. Hashimoto, Low temperature synthesis of Ti_3SiC_2 from Ti/SiC/C powders, Materials Science and Technology 20 (2004) 1252–1256.

[24] S. Yang, S.Z.M. Sun, Q. Yang, H. Hashimoto, Effect of Al addition on the synthesis of Ti_3SiC_2 bulk material by pulse discharge sintering process, Journal of the European Ceramic Society 27 (2007) 4807–4812.

[25] Y. Zou, Z.M. Sun, S. Tada, H. Hashimoto, Effect of Al addition on low temperature synthesis of Ti_3SiC_2 powder, Journal of Alloys and Compounds 461 (2008) 579–584.

[26] J.M. Cordoba, M.J. Sayagues, M.D. Alcala, F.J. Gotor, Synthesis of Ti_3SiC_2 powders: reaction mechanism, Journal of the American Ceramic Society 90 (2007) 825–830.

[27] E. Wu, E.H. Kisi, *In situ* neutron powder diffraction study of Ti_3SiC_2 analysis, Journal of the American Ceramic Society 84 (2001) 2281–2288.

[28] T. El-Raghy, M.W. Barsoum MW, Processing and mechanical properties of Ti_3SiC_2. Part I: reaction path and microstructure evolution, Journal of the American Ceramic Society 82 (1999) 2849–2854.

[29] K. Tang, C. Wang, Y. Huang, Q. Zan, X. Xu, A study on the reaction mechanism and growth of Ti_3SiC_2 synthesized by hot-pressing, Materials Science and Engineering: A 328 (2002) 206–212.

[30] M. Eizenberg, R. Brener, S.P. Murarka, Thermal stability of the aluminum/titanium carbide/silicon contact system, Journal of Applied Physics 55 (1984) 3799–3803.

[31] I. Barin, in: Thermochemical Data of Pure Substances, 3rd ed., Weinheim, New York, 1995.

[32] R. Pampuch, M. Raczka, J. Lis, The role of liquid phase in solid combustion synthesis of Ti_3SiC_2, International Journal of Materials and Product Technology 10 (1995) 316–324.

[33] F. Sato, J.F. Li, R. Watanabe, Reaction synthesis of Ti_3SiC_2 from mixture of elemental powders, Materials Transactions 41 (2000) 605–609.

[34] Y. Zou, Z.M. Sun, H. Hashimoto, L. Cheng, Reaction mechanism in Ti–SiC–C powder mixture during pulse discharge sintering, Ceramics International 36 (2010) 1027–1031.

[35] J.T. Li, Y. Miyamoto, Fabrication of monolithic Ti_3SiC_2 ceramic through reactive sintering of Ti/Si/2TiC, Journal of Materials Synthesis and Processing 7 (1999) 91–96.

[36] D. Riley, E. Kisi, T. Hansen, A. Hewat, Self-propagating high-temperature synthesis of Ti_3SiC_2: I, ultra-high-speed neutron diffraction study of the reaction mechanism, Journal of the American Ceramic Society 85 (2002) 2417–2424.

[37] C. Racault, F. Langlais, R. Naslain, Solid-state synthesis and characterization of the ternary phase Ti_3SiC_2, Journal of Materials Science 29 (1994) 3384–3392.
[38] T. El-Raghy, M.W. Barsoum, Diffusion kinetics of the carburization and silicidation of Ti_3SiC_2, American Institute of Physics 83 (1998) 112–119.
[39] N.F. Gao, Y. Miyamoto, K. Tanihata., Dense Ti_3SiC_2 prepared by reactive HIP, Journal of Materials Science 34 (1999) 4385–4392.
[40] J. Zhu, B. Mei, X. Xu, J. Liu, Synthesis of single-phase polycrystalline Ti_3SiC_2 and Ti_3AlC_2 by hot pressing with the assistance of metallic Al or Si, Materials Letters 58 (2004) 588–592.
[41] T. El-Raghy, M.W. Barsoum, A. Zavaliangos, S.R. Kalidindi, Processing and mechanical properties of Ti_3SiC_2: II, effect of grain size and deformation temperature, Journal of the American Ceramic Society 82 (1999) 2855–2860.